Food Chemistry: X 24 (2024) 101926

Contents lists available at ScienceDirect

Food Chemistry: X

journal homepage: www.sciencedirect.com/journal/food-chemistry-x

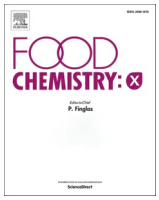

Electrostatically-enhanced two-stage low-temperature tempering: Effects on the quality of frozen tan mutton

Yuanlv Zhang , Guishan Liu *

College of Food Science and Engineering, Ningxia University, Yinchuan, Ningxia 750021, China

ARTICLE INFO

Keywords:
Two-stage low-temperature tempering
Electrostatic field assistance
Tempering methods
Tan mutton

ABSTRACT

The two-stage low-temperature tempering (TLT) and TLT assisted by electrostatic fields (TLT-1500/2000/2500/3000) were developed to investigate their effects on the quality of frozen Tan mutton. The results demonstrated that both TLT and TLT-1500/2000/2500/3000 significantly ($P < 0.05$) enhanced the tempering rate compared to refrigerator tempering (4 °C, RT). The analysis of tempering, cooking, and centrifugal losses, along with the evaluation of electrical conductivity, pH, and TVB-N, showed that the water retention capacity and freshness of Tan mutton treated with TLT-2500 were closest to those of fresh Tan mutton. Scanning electron microscopy analysis demonstrated that TLT-2500 best maintained the tissue integrity of Tan mutton, while low-field nuclear magnetic resonance analysis revealed it contained the highest immobile water and least free water. Furthermore, Tan mutton treated with TLT-2000 and TLT-2500 exhibited minimal lipid oxidation and color change. In contrast, the most significant changes in all indicators were observed after RT.

1. Introduction

Tan sheep is a valuable livestock species in Ningxia, renowned for its tender meat, and rich in high-quality protein, unsaturated fatty acids, essential vitamins, and various minerals, which provides significant health benefits (Zhang et al., 2024). During storage and processing, endogenous enzymes and spoilage microorganisms can utilize these nutrients, leading to undesirable changes in key quality characteristics such as color, texture, water-holding capacity, and nutritional value, ultimately affecting the overall eating quality and market value of Tan mutton (Zhang et al., 2023a). To ensure the freshness and safety of Tan mutton, freezing technology is commonly employed (Zhang et al., 2023b). Consequently, the thawing process becomes a crucial step before further processing (e.g., slicing, dicing) or direct cooking of frozen Tan mutton (Hu et al., 2021).

Traditionally, the thawing process is considered complete as the central temperature of a frozen meat product reaches 0 to 4 °C, allowing it to be boned or cut by hand (Zhu et al., 2021). Although the ideal goal of thawing is to bring the quality of frozen meat as close as possible to that of fresh meat, some of the water in frozen meat is lost as juices upon thawing, which carries away soluble nutrients, resulting in a loss of nutritional value (Zhang, Li, Jin, et al., 2021). Additionally, the increased temperature of thawed meat products accelerates microbial spoilage and enzymatic reactions, exacerbating the quality deterioration of the meat (Li, Zhao, et al., 2020). To address these issues, tempering was developed. Tempering is an incomplete stage of thawing, where the final temperature is −5 to −2 °C (Zhang, Li, Jin, et al., 2021). During this stage, the moisture in the meat product is in a transitional state from solid to liquid (Llave & Erdogdu, 2022). Tempering effectively reduces the risk of juice and nutrient loss compared to conventional thawing (Zhu et al., 2019). The lower final temperatures also inhibit the growth of spoilage microorganisms, lipid and protein oxidation, and other factors that may negatively affect the quality of meat products (Wang et al., 2023). Furthermore, the market size for prepared foods, especially prepared meat products, is rapidly expanding. Tempered raw meat better maintains the textural characteristics and basic morphology of near-solid states, aligning well with the processing performance requirements (mechanized cutting and processing) emphasized in the industrial production of prepared meat products.

Interestingly, low temperatures are effective in inhibiting microbial spoilage and reducing meat deterioration; however, it is evident that low temperatures can also significantly affect the thawing rate of frozen meat and lead to lipid and protein oxidation. Conversely, fluctuating temperatures can promote heat exchange, potentially increasing the thawing rate and reducing lipid and protein oxidation (Zhu et al., 2021). Lee et al. (2021) investigated the effect of two-stage air thawing (25 °C/

* Corresponding author.
E-mail address: liugs@nxu.edu.cn (G. Liu).

https://doi.org/10.1016/j.fochx.2024.101926
Received 18 September 2024; Received in revised form 21 October 2024; Accepted 23 October 2024
Available online 24 October 2024

−1.5 °C, 25 °C/2 °C) on the thawing time and quality of frozen pork. They found that two-stage air thawing, compared to constant temperature air thawing (−1.5 °C, 2 °C, and 25 °C), not only significantly reduced the total thawing time but also effectively inhibited lipid oxidation and protein degradation, and maintained better moisture-related properties. Similar findings were also reported by Li et al. (2014), Zhu et al. (2021), and Zhu et al. (2023), indicating that fluctuating temperatures held great potential for meat thawing applications. Additionally, the electrostatic field, an emerging non-thermal processing technology, is characterized by high thawing efficiency, good quality of thawed meat, low energy consumption, and simple equipment requirements (Mousakhani-Ganjeh et al., 2016a). Therefore, its application in the thawing process of frozen meat products has garnered increasing attention. Jia, Liu, et al. (2017) reported that the thawing efficiency of rabbit meat in an electrostatic field of −15, −20, or − 25 kV was significantly ($P < 0.05$) higher than that of conventional air thawing, with the high-voltage electrostatic field (HVEF) treatment resulting in a 0.5–1.7-log reduction in microbial population. Subsequent studies have applied the electrostatic field thawing technique to various frozen meats such as chicken breast protein (Rahbari et al., 2018), and pork tenderloin (Jia et al., 2020), demonstrating similar benefits.

At present, the effect of two-stage low-temperature tempering (TLT) assisted by an electrostatic field on the quality of frozen Tan mutton has rarely been reported. Therefore, in this study, TLT, TLT assisted by an electrostatic field (TLT-1500/2000/2500/3000), and traditional refrigerator tempering (RT) was used to investigate the effects of these various tempering approaches on the quality indices of water retention capacity, freshness, physical characteristics, moisture distribution and migration, lipid oxidation, and color change of Tan mutton, with fresh Tan mutton (FM) serving as a control. This study aims to provide theoretical and technical support for the application of electrostatic field-assisted TLT in the processing industry of Tan mutton.

2. Material and methods

2.1. Sample preparation

The mutton obtained from a batch of seven ten-month-old Tan sheep were purchased in a local slaughterhouse in Yinchuan, China. The mutton was cooled and aged at the slaughterhouse before being transported to our laboratory within a three-hour window. The visible fat and connective tissue on the mutton were removed, and then cut into pieces of 40 mm × 40 mm × 50 mm. A total of 21 samples were randomly divided into seven groups after inserting a type K thermocouple (Yuyao Gongyi Meter Co., Ltd., Yuyao, Zhejiang, China). Except for one group (FM) for analysis immediately, the remaining six groups of samples were rapidly subjected to ultra-low temperature freezing in a − 80 °C freezer (DW-86 L579, Haier Biomedical Co., Ltd., Qingdao, Shandong, China) until the central temperature decreased to −20 °C. Subsequently, they were transferred to a − 20 °C refrigerator for further storage for a minimum of 48 h before subsequent tempering procedures. Each sample was individually packed in a separate PE bag to prevent water loss during freezing and storage.

2.2. Tempering methods

The tempering system is depicted in Supplementary material 1, while the TLT, TLT-1500/2000/2500/3000, and RT are referenced from our preceding research (Zhang et al., 2024).

2.3. Time-temperature profile

Temperature data throughout the tempering process were obtained from a type K thermocouple integrated within the tempering system, with temperature readings recorded at one-minute intervals. After the completion of the tempering process, a temperature-time curve was constructed.

2.4. Water retention capacity (WRC)

2.4.1. Tempering loss

The tempering loss was determined using the method reported by Wang et al. (2023), with slight modifications. The weight of the Tan mutton before tempering was accurately measured with an analytical balance and recorded as m_1. Following completion of tempering, the mutton surface was dried with absorbent paper and reweighed, recorded as m_2. The tempering loss was calculated using Eq. (1-1):

$$\text{Tempering loss} = \frac{m_1 - m_2}{m_1} \times 100\% \quad (1\text{-}1)$$

2.4.2. Cooking loss

Cooking loss was determined following the method reported by Zhu et al. (2019), with minor modifications. The weight of the tempered mutton was accurately measured using an analytical balance and recorded as m_3. Subsequently, the mutton was steamed with water vapor for 5 min, cooled to room temperature surface water wiped off with absorbent paper, and reweighed, recorded as m_4. The cooking loss was calculated using Eq. (1-2):

$$\text{Cooking loss} = \frac{m_3 - m_4}{m_3} \times 100\% \quad (1\text{-}2)$$

2.4.3. Centrifugal loss

The method described by Zhou and Xie. (2021) was applied to determine centrifugal loss with slight modifications. A section of the Tan mutton measuring 10 × 10 mm^2 in cross-section was cut, accurately weighed, and recorded as m_5. Subsequently, the mutton was wrapped with two pieces of filter paper, loaded into a 50 mL centrifuge tube, and centrifuged at 4 °C and 5000 r/min for 10 min. After peeling off the filter paper, the weight of the sample was accurately measured and recorded as m_6. Centrifugal loss was calculated using Eq. (1-3):

$$\text{Centrifugal loss} = \frac{m_5 - m_6}{m_5} \times 100\% \quad (1\text{-}3)$$

2.5. Freshness of tan mutton

2.5.1. Electrical conductivity (EC)

The EC was determined following the method reported by Zhang, Cao, Shi, and Cai (2021) with minor modifications. Specifically, 3 g of the tempered mutton was obtained, finely chopped, and subsequently immersed in 30 mL of distilled water, left to equilibrate at room temperature for 30 min. The resulting mixture was then subjected to centrifugation at 1500 ×g for 5 min, after which the EC of the supernatant was measured using a conductivity meter.

2.5.2. pH

The pH was determined by referring to the method reported by Lan et al. (2021), with slight modifications. Specifically, 10 g of tempered and minced lamb was weighed and combined with 100 mL of deionized water, followed by homogenization for 2 min using a homogenizer at 5000 r/min. After allowing the mixture to stand at room temperature for 30 min, the pH of the resulting supernatant was measured using an acidimeter.

2.5.3. Total volatile base nitrogen (TVB-N)

The TVB-N content of Tan mutton was determined using an Automatic Kjeldahl apparatus (Hanon K9860, China). 10 g of chopped mutton and 1 g of magnesium oxide were weighed and transferred into a 750 mL digestion tube. TVB-N was quantified following standard procedures, with results reported in mg /100 g.

2.6. Scanning electron microscope (SEM)

The SEM analysis was conducted with minor modifications following the method delineated by Jia, He, et al. (2017). Samples were sectioned into dimensions of 3 × 3 × 2 mm^3, then immersed in a pH 7.2, 2.5 % (*v*/v) glutaraldehyde solution (containing 10 mM Tris-HCl and 0.6 M NaCl) for 24 h. Subsequently, the samples underwent a gradient elution process with varying concentrations of ethanol (50 %, 60 %, 70 %, 80 %, and 90 %), each for 10 min. Following dehydration three times with anhydrous ethanol for 10 min per treatment, the samples were affixed to conductive adhesive tape, sputter-coated with gold, and observed for surface structural characteristics using SEM at an accelerating voltage of 3.0 kV and a magnification factor of 500×.

2.7. Moisture distribution and migration

A low-field nuclear magnetic resonance analyzer (LF-NMR) was employed to evaluate the distribution and migration of moisture within Tan mutton, following the method reported by Wang et al. (2022). After equilibrating at room temperature for 30 min, the mutton was sectioned into rectangular prisms with dimensions of 10 × 10 × 20 mm^3 and subsequently positioned into a 15 mm diameter NMR sample tube. The T_2 relaxation time signals were acquired using the Carr-Purcell-Meiboom-Gill (CPMG) pulse sequence. The parameters were configured as follows: SF (MHz) = 18, P1 (μs) = 17, TW (ms) = 3000, P2 (μs) = 33, NECH = 2500, TE (ms) = 0.26, SW (KHz) = 200, RFD (ms) = 0.200, RG1 (db) = 20.0, DRG1 = 3, DR = 1, and NS = 8. Data inversion was performed using LF-NMR software.

2.8. Lipid oxidation

Lipid oxidation in Tan mutton was determined using a Malondialdehyde (MDA) Colorimetric Assay Kit (*E*-BC-K025-S, Elabscience Biotechnology Co., Ltd.). The thiobarbituric acid reactive substances (TBARS) values were determined using MDA as a standard, the assay method followed the instructions of the kit and the results were expressed in terms of protein quantity.

2.9. Color and luster

The L^*, a^*, *and* b^* of Tan mutton were measured using a colorimeter, following the procedure described by Li et al. (2021). Before each measurement, calibration was performed using a white standard plate.

2.10. Statistical analysis

One-way analysis of variance (ANOVA) was used to analyze data following a Tukey's multiple comparison, expressed as mean ± standard deviation (SD) (SPSS 22.0, Chicago, IL, USA), and the confidence interval was set at 95 % ($P < 0.05$). All graphs were generated using Origin 2022. All measurements were carried out in triplicate.

3. Results and discussion

3.1. Time-temperature profile analysis

The time-temperature profiles of the tempering process were illustrated in Fig. 1. Results indicated that all tempering strategies take less than 50 min to traverse the range from −18 to −5 °C. The stage characterized by the most significant discrepancy in total tempering time lies between −5 to −2 °C, which corresponds to the zone of maximum ice crystal formation (Sun et al., 2021). This reduction in tempering rate is attributed to the absorption of energy during the ice-water phase transition process in frozen foods, without a concurrent rise in temperature (Zhang, Li, Yao, et al., 2021). Furthermore, tempering treatment leads to preferential melting of the surface layer of the sample, gradually transferring energy to the central region. However, the presence of the molten layer with lower thermal conductivity reduces the rate of heat transfer, resulting in slower heating rates (Chen et al., 2020).

Compared with the RT (4 °C, 297 min), TLT significantly shortened the tempering duration (258 min, $P < 0.05$). On the one hand, the limited heat transfer coefficient of air hindered rapid heat transfer (Yao et al., 2023). TLT, on the other hand, involved elevating the tempering temperature (4 °C → 8 °C) after entering the maximum ice crystal formation zone, thereby increasing the temperature differential between

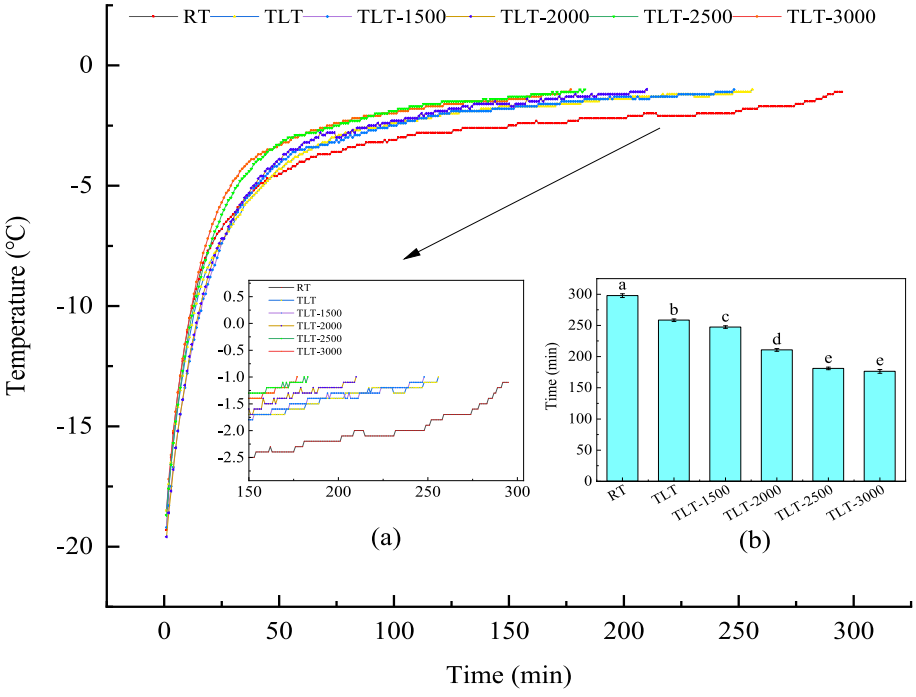

Fig. 1. Temperature-time profiles of tan mutton under diverse tempering approaches. Different lowercase letters indicate significant differences ($P < 0.05$), while error bars show standard deviation.

the tempering environment and the sample, facilitating swift traversal through this region. Moreover, TLT assisted by electrostatic field significantly reduced the tempering time ($P < 0.05$), with a corresponding increase in the applied electrostatic field intensity. This is attributed to the micro-energy generated by the electrostatic field, which accelerates the disruption of hydrogen bonds within the ice structure, leading to the formation of smaller ice crystals transitioning gradually into a liquid state of small molecular water. Additionally, the electrostatic field accelerates the motion of charged particles, inducing an ionic wind (Rahbari et al., 2018). Upon collision with the ice surface, these fast-moving charged particles transfer energy to water molecules, which in turn increases the kinetic energy of the water molecules, accelerating their melting (Li, Shi, et al., 2020). Simultaneously, the deposition of these charged particles on the ice surface enhances thermal conductivity, facilitating quicker heat absorption from the surroundings and enhancing melting speed (Jia et al., 2020). As the electrostatic field intensity increased, collisions between charged particles and air molecules increased, generating new charged particles. Additionally, the velocity of particle motion increased with higher electrostatic field intensity, resulting in a notable enhancement in heat transfer efficiency and a significant reduction in duration through the maximum ice crystal formation zone ($P < 0.05$). However, beyond an electric field strength of 2500 V, tempering efficiency did not increase significantly ($P > 0.05$). This could be attributed to the saturation of the ionic wind intensity formed by charged particles within a certain space, limiting further acceleration of ice crystal melting.

3.2. WRC

3.2.1. Tempering loss

The tempering loss is intricately linked to the WRC of muscle, which consequently impacts the structural integrity of muscle tissue and the organoleptic properties of meat (Cai et al., 2019). Intracellular and extracellular ice crystals formed in Tan mutton after freezing present a significant challenge to myocyte integrity and may induce mechanical damage to muscle tissue (M. Cao et al., 2018). Furthermore, the tempering inevitably hastens the denaturation, aggregation, and degradation of proteins, significantly diminishing their ability to bind water molecules, ultimately leading to tempering loss.

The tempering loss of mutton following various tempering was illustrated in Fig. 2. The RT exhibited the most pronounced tempering loss (2.62 %), whereas TLT-2500 resulted in the least tempering loss (0.62 %). Considering the oxidative denaturation of MPs as discussed by Zhang et al. (2024), it became apparent that prolonged tempering duration at RT led to extensive denaturation and degradation of MPs which were crucial for maintaining WRC in muscle tissues, losing their functionality in water binding and reabsorption. Consequently, the substantial water loss not only entailed the depletion of water-soluble and sarcoplasmic proteins but also detrimentally impacted the organoleptic and palatability attributes of mutton. The analysis of SEM of mutton in Section 3.4, along with color and luster in Section 3.7, further corroborated these observations. Furthermore, the application of TLT and electrostatic fields significantly expedited the tempering process ($P < 0.05$) and mitigated the oxidative denaturation of MPs. The staged warming strategy of TLT facilitated rapid traversal through the zone of maximum ice crystal formation, thereby averting structural damage to mutton tissue caused by large ice crystals.

Conversely, the micro-energetic effect of the electrostatic field expedited the transformation of mutton ice crystals into small-molecule water, thus preventing the formation and destruction of large ice crystals. As depicted in Fig. 2, the tempering loss of mutton progressively decreased with increasing electrostatic field intensity, reaching its nadir at TLT-2500. However, when electrostatic field strength was raised to 3000 V (TLT-3000), mutton tempering loss exhibited a significant rebound ($P < 0.05$), potentially due to excessive oxidative stress and diminished MPs-water molecule binding capacity (Zhu et al., 2021). Moreover, the tempering rate peaked at TLT-3000, likely impeding timely water absorption by muscle tissues. Among all tempering methods, TLT-2500 demonstrated the lowest tempering loss, indicating effective preservation of muscle tissue integrity, stabilization of MPs physicochemical properties, and reduced juice loss during tempering, thereby representing the optimal strategy for water retention.

3.2.2. Cooking loss

Cooking loss stands as a pivotal metric indicative of muscle WRC. As meat samples transition from raw to cooked, MPs undergo thermal denaturation at elevated temperatures, leading to the disruption of muscle organizational structure. Consequently, water and soluble

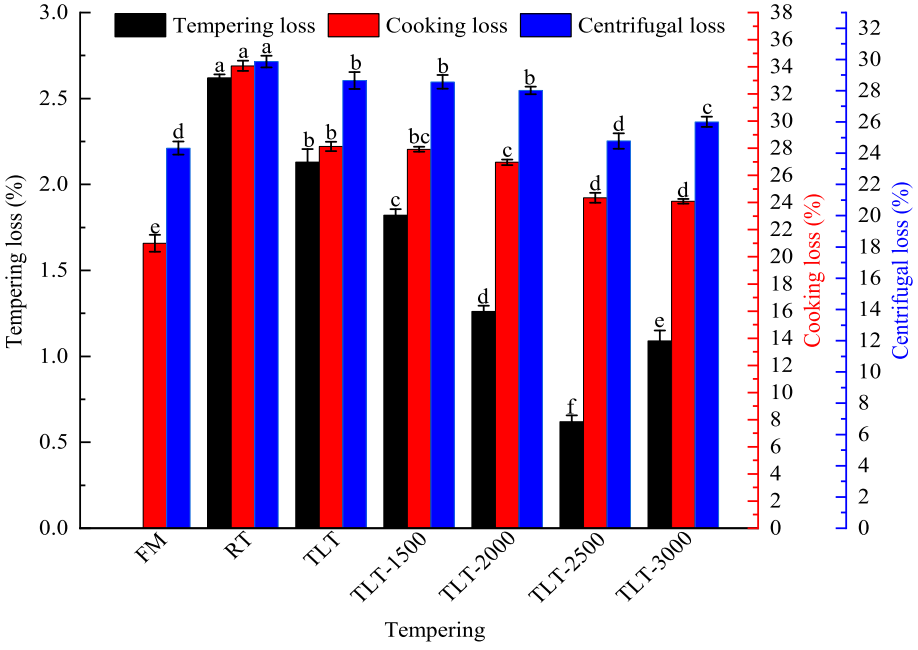

Fig. 2. Changes in water retention capacity (tempering loss, cooking loss, and centrifugal loss) of tan mutton under different tempering treatments. Different lowercase letters indicate significant differences ($P < 0.05$), while error bars show standard deviation.

substances are liberated from interstitial spaces and muscle tissues, culminating in cooking loss (Cheng et al., 2022). Variations in water tethering capacity, gauged through water loss measurements in Tan mutton, exhibited a significant and negative correlation with desirable eating qualities such as juiciness. Hence, reduced cooking losses may translate to enhanced eating experiences. Fig. 2 presents the outcomes delineating the impact of diverse tempering methods on Tan mutton cooking loss.

FM exhibited the lowest cooking loss (21.00 %), whereas tempering treatments significantly ($P < 0.05$) elevated the cooking loss of Tan mutton across all groups. RT exhibited the highest cooking loss (34.07 %), whereas TLT-2500 (24.34 %) and TLT-3000 (24.09 %) demonstrated cooking losses closest to FM. Cooking loss of Tan mutton progressively diminished with TLT and electrostatic field application, mirroring the trend observed in tempering loss (Fig. 2). SEM analyses (Section 3.4) further corroborate that Tan mutton treated with TLT-2500 and TLT-3000 retained moisture at elevated temperatures, exhibited superior muscle tissue integrity, and presented favorable eating quality. However, Lv and Xie (2022) reported that when thawing tuna at 4 °C, similar cooking losses to the latter two were obtained ($P > 0.05$), despite consuming tens of times as much time as ultrasound and microwave. Similar results were also reported by Zhou and Xie. (2021). There may be several reasons for the differences between the above studies and the present study: firstly, it may lie in the differences in the objects to be thawed, especially the differences in volume and heat transfer between fish products and the Tan mutton (livestock products) studied in this paper. Additionally, disparities in cooking losses might arise from the choice of thawing method; microwave and ultrasound techniques were associated with greater structural damage to muscle tissue and MP compared to RT, leading to higher cooking losses. Moreover, when samples undergo rapid freezing, the volume of water molecules within cells undergoes rapid changes, leading to the generation of internal stresses. A mismatch between the thawing rate and the change in internal stress results in further rapid changes in cell volume and the generation of new internal stresses, rendering the cell more susceptible to destruction (Li, Zhao, et al., 2020). Conversely, with slower thawing rates, stresses within the cell become more balanced and uniform, preserving cell integrity more effectively (Lan et al., 2021). Thus, although ultrasound and microwave techniques expedite thawing, they also induced drastic changes in intracellular water molecules, heightening internal stresses and cellular damage. In contrast, RT, despite its prolonged thawing duration, maintains intracellular stress equilibrium, safeguarding cellular structural integrity and resulting in relatively low juice loss.

3.2.3. Centrifugal loss

Centrifugal loss is commonly employed to characterize the capacity of muscle tissue to retain water by physically entrapping it, and the water content in muscle is predominantly intracellular. During tempering, when proteins undergo denaturation due to heat or force fields and cells suffer damage or rupture from ice crystals or internal stresses, intracellular water migrates to intercellular or extracellular spaces, forming juice (Lv & Xie, 2022). This juice is subsequently subject to centrifugal loss under external forces, such as centrifugal force.

As shown in Fig. 2, FM exhibited the lowest centrifugal loss (24.33 %), with TLT-2500 (24.78 %) showing no significant difference in centrifugal loss compared to FM ($P > 0.05$). Conversely, RT, TLT, TLT-1500, TLT-2000, and TLT-3000 experienced elevated centrifugal losses by 22.73 %, 17.80 %, 17.38 %, 15.17 %, and 6.90 %, respectively, compared to FM, indicating that tempering treatments induced a degree of tissue damage in Tan mutton. Particularly, RT exhibited the most pronounced increase in centrifugal loss. This can be attributed to the longer tempering duration of RT compared to TLT and electrostatic field treatments, resulting in gradual sample warming and more severe denaturation of MPs, which fail to retain hydration efficiently, leading to centrifugal loss, consistent with findings reported by (Zhou & Xie., 2021).

Conversely, TLT and electrostatic field treatments expedited the passage of mutton samples through the zone of maximum ice crystal formation (−5 °C to −2 °C), hindering the proliferation of spoilage microorganisms and oxidative denaturation of MPs to some extent. Consequently, muscle cells-maintained morphology better and retained intracellular water, resulting in a milder centrifugal loss. Additionally, centrifugal loss of mutton diminished progressively with increasing electrostatic field strength. This phenomenon might be attributed to the accelerated tempering process induced by higher electrostatic field strength, which inhibits ice crystal growth, reduces structural damage to muscle cells, and preserves cell WRC (Hu et al., 2021). Moreover, the non-thermal processing characteristic of the electrostatic field mitigates excessive oxidative denaturation of MPs, thereby minimizing the impact on protein-water hydration.

3.3. Freshness of tan mutton

3.3.1. EC

EC stands as a crucial parameter indicating the freshness of muscle foods. During the spoilage process, proteins and fats in muscle foods degrade into smaller molecules under the influence of exogenous microbial proteases, forming ions that contribute to the formation of numerous mobile conductive compounds, thus augmenting solution conductivity (Zhou & Xie., 2021). Consequently, EC serves as a proxy for the freshness of muscle foods and exhibits an inverse relationship with it.

Fig. 3 illustrated that FM displayed an EC of 1.39 mS/cm, while RT, TLT, TLT-1500, TLT-2000, TLT-2500, and TLT-3000 exhibited EC of 1.80, 1.68, 1.59, 1.48, 1.51, and 1.54 mS/cm, respectively. The highest EC in RT likely attributed to prolonged treatment duration. The extended RT treatment allowed for higher microbial degradation of nutrients such as proteins and fats, yielding increased ion production. This is supported by the analysis of TVB-N in Section 3.3.3 and lipid oxidation (TBA) in Section 3.6, indicating a positive correlation between EC, TVB-N, and TBA. Additionally, the analysis of WRC in Section 3.2 revealed that RT induced higher juice loss, leading to the migration of intracellular water to extracellular/muscular interstitial spaces, resulting in elevated water content and EC (Cai et al., 2019). Similarly, Zhang, Cao, Shi, and Cai (2021) reported that longer thawing times with ultrasound (400 W, 40 kHz) and far-infrared (300 W) resulted in increased water migration, converting intracellular water into free water, consequently elevating EC ($P < 0.05$). Conversely, combining ultrasound with microwave or far-infrared, with thawing times less than 1/3 of ultrasound thawing time, yielded lower EC (868.95 μS/cm and 870.15 μS/cm, respectively). TLT and electrostatic field strategies markedly accelerated the tempering process ($P < 0.05$), resulting in reduced air contact for Tan mutton, minimizing protein denaturation and lipid oxidation, thereby yielding relatively low EC, as also concluded by Zhu et al. (2021). Furthermore, as electrostatic field strength increased, mutton EC gradually decreased, reaching its nadir at TLT-2000. This trend aligns with the effects of different tempering methods on water migration (Section 3.5), lipid oxidation (Section 3.6), and MP denaturation (Zhang et al., 2024) in Tan mutton.

3.4. pH

pH is one of the important indicators of muscle food quality, intimately linked to changes in attributes such as color, water retention, texture, and flavor. As depicted in Fig. 3, the pH of fresh Tan mutton stood at 6.15, while RT, TLT, TLT-1500, TLT-2000, TLT-2500, and TLT-3000 treatment groups exhibited pH values of 5.47, 5.65, 5.56, 6.07, 6.13, and 6.00, respectively. pH values in all groups, except TLT-2500, were significantly lower ($P < 0.05$) compared to fresh Tan mutton. The pH decline can be attributed to several factors: Firstly, muscle cells undergo ongoing glycogenolysis and phosphocreatine degradation

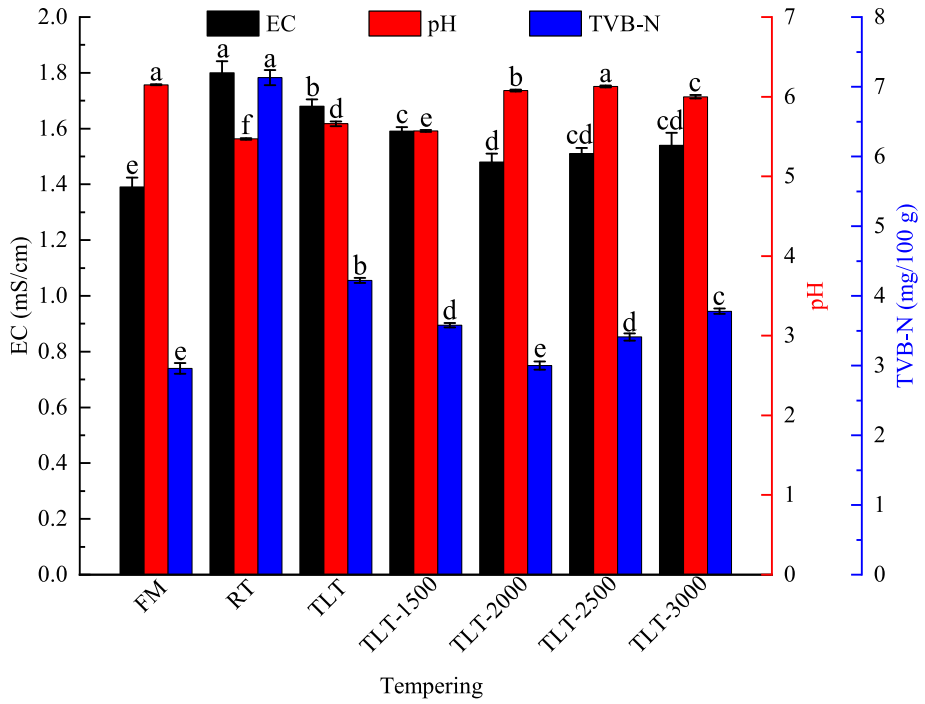

Fig. 3. Changes in freshness (EC, pH, and TVB-N) of tan mutton under different tempering treatments. Different lowercase letters indicate significant differences ($P < 0.05$), while error bars show standard deviation.

reactions during tempering treatment, leading to the accumulation of acids such as PO3–4 (Du et al., 2022). Secondly, juice loss during tempering may result in the depletion of minerals, small-molecule proteins, and other constituents from the muscle, disturbing ionic equilibrium and subsequently lowering pH (Zhang et al., 2024).

In conjunction with the analysis of the WRC of Tan mutton in Section 2.4, the pH variation closely correlates with the water tethering force of the muscle. The impact of pH on muscle WRC fundamentally stems from the electrostatic charge effect of protein molecules (Du et al., 2022). On one hand, electrostatic charge serves as the driving force for protein molecules to attract water molecules for hydration. Simultaneously, it enhances electrostatic repulsion between protein molecules, thereby loosening their structure and creating space for water accommodation (M. Cao et al., 2018). During the acceleration of the tempering process by TLT and electrostatic field, the decomposition of muscle proteins into peptides, amino acids, and amines by tissue proteases slows down, leading to deviation from the isoelectric point of muscle protein (Lv & Xie, 2022). This expands spatial structure and polar attraction, ultimately enhancing meat water retention. Furthermore, TLT and electrostatic field treatments may affect ATPase activity due to faster tempering rates, slowing down ATP consumption and actin formation. This results in a significant increase in the effective gap between myosin and actin, further influencing sample water retention (Cai et al., 2020). Conversely, the prolonged tempering time of RT leads to a decrease in pH, nearing the isoelectric point of muscle protein. This weakens electrostatic repulsion between proteins, causing structural tightening. Consequently, the spaces between protein molecules for water accommodation decrease, diminishing muscle water retention. Additionally, as pH approaches the isoelectric point of muscle protein, protein gravitational force for water hydration decreases, myofibril interstitial space contracts, and muscle water retention correspondingly weakens (Cheng et al., 2022).

3.4.1. *TVB-n*

The TVB-N is a collective term encompassing alkaline nitrogenous substances such as ammonia and amines. These compounds arise from endogenous enzymes and microbial breakdown of proteins and non-protein nitrogenous compounds (e.g., amino acids and nucleotides) during the spoilage of muscle foods (Lan et al., 2021). Consequently, TVB-N serves as a crucial marker for assessing the freshness of muscle foods, exhibiting an inverse correlation with their freshness levels. The TVB-N of Tan mutton following various tempering methods are depicted in Fig. 3. The FM exhibited a TVB-N of 2.96 mg/100 g, whereas the values for each tempering group—RT, TLT, TLT-1500, TLT-2000, TLT-2500, and TLT-3000—stood at 7.13, 4.22, 3.58, 3.00, 3.41, and 3.78 mg/100 g, respectively. This indicates that, except for TLT-2000, the TVB-N significantly increased in the remaining groups ($P < 0.05$). Such elevation can be attributed to microbial proliferation on the tempered Tan mutton and the concomitant impact of microbial and cellular autolysis (endogenous enzymes), resulting in the degradation of proteins and non-protein nitrogen compounds (Bekhit et al., 2021). Nonetheless, it is noteworthy that all samples exhibited TVB-N values below 15 mg/100 g, thus remaining within the standard limit for fresh meat.

A higher TVB-N in RT may be attributed to the prolonged duration of tempering, leading to excessive protein degradation and heightened production of ammonia and amines (Cai et al., 2020). The application of TLT and electrostatic fields significantly ($P < 0.05$) reduced the TVB-N content in mutton. This reduction could be attributed to the shorter tempering time associated with all tempering methods, maintaining the Tan mutton at a high level of freshness and effectively preventing microbial reproduction (Hu et al., 2021). Additionally, as the electrostatic field intensity increased, the TVB-N content in Tan mutton further decreased until it exhibited no significant difference from fresh Tan mutton, particularly evident in TLT-2000 ($P > 0.05$). This phenomenon can be attributed to the ozone and negative air ions generated by corona discharge around the electrodes, which reduce spoilage and pathogenic bacteria (Mousakhani-Ganjeh et al., 2016b). With increased electric field strength, corona discharge intensifies, leading to enhanced inhibition of spoilage microorganisms and reduced TVB-N content in Tan mutton (J. Li et al., 2020). However, when electrostatic field strength exceeded 2000 V, TVB-N values in Tan mutton began to rebound and rise. This rebound may stem from severe oxidative denaturation of MPs and exposure of more proteolytic sites at higher field strengths (Qian et al., 2019). Consequently, heightened exposure to proteolytic sites

allows free proteases generated during tempering to work at ultra-high efficiency, facilitating the degradation of macromolecular proteins into small-molecule polypeptides or oligopeptides (Zhang et al., 2023b). Hence, although ozone generated by high-intensity electrostatic fields exhibits a pronounced effect on inhibiting spoilage microorganisms, these microorganisms efficiently utilize protein degradation products, i.e., small molecule polypeptides or oligopeptides. Ultimately, this interplay between endogenous proteases and spoilage microorganisms contributes to the elevation of TVB-N values in Tan mutton.

3.5. SEM

The integrity of myofibrils correlates closely with quality indicators such as water retention, tenderness, and color of the muscle; specifically, denser interstitial structures between myofibrils and smaller myofibrillar gaps correspond to improved tenderness and water retention of the muscle (Hu et al., 2021). Fig. 4 illustrated the effects of different tempering methods on the microstructure of Tan mutton. Fresh Tan mutton exhibited neatly arranged, tightly interstitial, longitudinally parallel muscle fiber structures throughout its length, with intact endomysium and myofascial membranes possessing smooth surfaces. This elastic muscle bundle membrane contributes to maintaining the integrity of muscle tissue and the dense arrangement of muscle fiber bundles (Li et al., 2019).

However, after tempering, the myogenic fiber structure of the muscle lost integrity, myofibrillar membranes sustained damage, and interstitial spaces within muscle bundles expanded, leading to increased water leakage, decreased muscle water retention, significant juice loss, and reduced tenderness. Notably, RT-induced muscle fiber fracture and delamination were particularly pronounced, with straight myofiber bundles exhibiting severe curling and contraction. Additionally, the originally smooth and flat myofiber bundles displayed substantial membrane rupture (connective tissue), severely compromising muscle tissue integrity and resulting in complete microstructure loss. This observation aligns with the findings of Hu et al. (2021). RT-induced muscle tissue deterioration may be attributed to prolonged tempering, exposing mutton tissues directly to the environment, fostering spoilage microorganism proliferation, protein decomposition, and consequent disruption of muscle tissue integrity, leading to loss of the original muscle fiber structure (Lan et al., 2021). Furthermore, the slow tempering rate of RT and ice crystal formation may gradually compromise muscle fiber integrity with prolonged tempering. During tempering, some ice crystals may melt due to heat absorption initially, and since the air pressure of liquid water vapor exceeds the water vapor pressure of ice crystals, the liquid-phase water melted by ice crystals accumulates in the interstitial space of tissue fibers at low pressure, increasing the interstitial pressure of Tan mutton tissues (Lv & Xie, 2022). Consequently, shear fragmentation induced by this pressure exacerbates tissue structure looseness and fragmentation. Additionally, prolonged RT may cause severe oxidation and denaturation of muscle proteins, reducing protein hydration capacity, followed by myogenic fiber structural fractures, enlargement of interstitial gaps in muscle fiber bundles, and even curling and fracture, ultimately resulting in substantial juice loss (Peng et al., 2021).

After TLT and electrostatic field tempering, the muscle bundle gap in Tan mutton tissue slightly enlarged, and muscle fibers exhibited fracture phenomena, resulting in poorer structural integrity of the endomembrane and muscle bundle membrane, consequently yielding a rougher muscle surface. However, with increased electrostatic field strength, the structural integrity of Tan mutton tissue showed slight improvement.

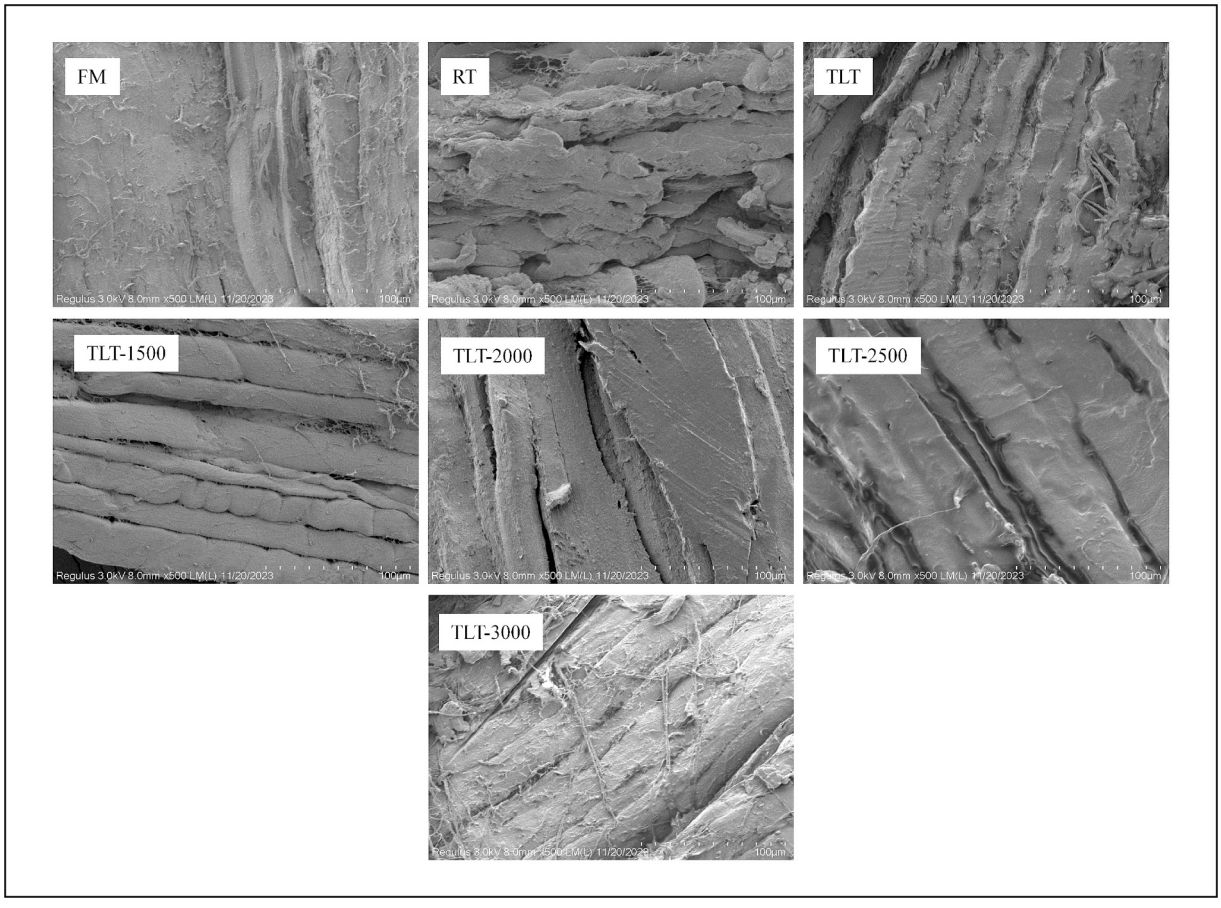

Fig. 4. Changes in micro-structure of tan mutton under different tempering treatments (×500).

Notably, at TLT-2000, the structural integrity of Tan mutton meat tissues closely resembled that of FM, featuring a flatter, more compact surface, neatly aligned myofibrils, and tighter, more consistent muscle bundle gaps. These tissue changes may be attributed to the rapid and uniform rate of TLT and electrostatic field tempering. A similar result was also reported by Qian et al. (2019).

3.6. Moisture distribution and migration

Water in muscle foods manifests in three primary forms: bound water, immobile water, and free water. Presently, low-field nuclear magnetic resonance (LF-NMR) techniques are extensively employed to scrutinize water distribution and migration in food products, delineating shifts in the three distinct water types via the decay pattern of transverse relaxation time (T_2) of ^{1}H proton in meat products. As depicted in Fig. 5, three characteristic T_2 peaks emerge within the range of 0 to 1000 ms: the 0 to 10 ms peak (T_{21}) denotes bound water, the 10 to 100 ms peak (T_{22}) represents immobile water, and the 100 to 1000 ms peak (T_{23}) indicates free water (Cai et al., 2019). Additionally, the peak area occupancies corresponding to these peaks are denoted as P_{21}, P_{22}, and P_{23}, respectively.

Table 1 illustrated variations in relaxation time and the corresponding moisture content of Tan mutton subjected to different tempering treatments. Minimal disparity was observed in T_{21} between FM and Tan mutton in each tempering group, with no significant alteration in P_{21} values noted ($P > 0.05$). Thus, bound water in Tan mutton appears largely unaffected by freezing and tempering (Lan et al., 2021). Subsequently, we examined changes in relaxation times (T_{22} and T_{23}) and peak areas (P_{22} and P_{23}) exclusively for immobile and free water. Compared to FM (T_{22} = 43.42 ms), the T_{22} values of RT, TLT, TLT-1500, TLT-2000, TLT-2500, and TLT-3000 increased by 97.19 %, 85.28 %, 77.91 %, 39.66 %, 46.13 %, and 46.13 % in each respective tempering group, indicating a loss of immobile water in Tan mutton. Similarly, the T_{23} values of RT, TLT, TLT-1500, TLT-2000, TLT-2500, and TLT-3000 significantly increased from 258.25 ms in FM to 493.19 ms, 442.79 ms, 350.74 ms, 319.75 ms, 336.14 ms, and 460.66 ms ($P < 0.05$), respectively, post-tempering, suggesting a loss of immobile water in Tan mutton and an increase in free water. Notably, T_{22} and T_{23} values for TLT-2000 and TLT-2500 closely approximated those of FM, indicative of tighter water binding and superior moisture retention in Tan mutton (Lv & Xie, 2022).

From Table 1, it is evident that P_{22} decreased from 91.87 % in FM to 88.44 %, 89.53 %, 91.24 %, 90.58 %, 91.29 %, and 90.44 % in RT, TLT, TLT-1500, TLT-2000, TLT-2500, and TLT-3000, respectively, post-tempering, while P_{23} increased from 5.29 % to 8.51 %, 7.63 %, 6.13 %, 6.15 %, 5.50 %, and 6.36 %, respectively. This trend reflects a gradual reduction in the relative content of immobile water and a corresponding increase in free water in FM following tempering. P_{22} and P_{23} for TLT-2500 were significantly higher and lower ($P < 0.05$) than those of other tempering groups, aligning closely with FM levels. This underscores TLT-2500 superior retention of immobile water and

Table 1
Effect of different tempering treatments on LF-NMR relaxation times (T_2) and peak ratios of tan mutton.

Tempering	T_2/ms			Proportion/%		
	T_{21}	T_{22}	T_{23}	P_{21}	P_{22}	P_{23}
FM	1.95 ± 0.08^{b}	43.42 ± 0.01^{f}	258.25 ± 17.99^{d}	2.84 ± 0.06^{ab}	91.87 ± 0.04^{a}	5.29 ± 0.08^{d}
RT	1.99 ± 0.06^{ab}	85.62 ± 0.06^{a}	493.19 ± 11.67^{a}	3.05 ± 0.22^{ab}	88.44 ± 0.24^{e}	8.51 ± 0.23^{a}
TLT	2.00 ± 0.03^{ab}	80.45 ± 0.02^{b}	442.79 ± 20.89^{b}	2.84 ± 0.27^{ab}	89.53 ± 0.27^{d}	7.63 ± 0.11^{b}
TLT-1500	2.10 ± 0.02^{a}	77.25 ± 0.03^{c}	350.74 ± 20.83^{c}	2.62 ± 0.10^{b}	91.24 ± 0.11^{b}	6.13 ± 0.07^{c}
TLT-2000	2.06 ± 0.03^{ab}	60.64 ± 0.02^{e}	319.75 ± 16.53^{c}	3.26 ± 0.05^{a}	90.58 ± 0.13^{c}	6.15 ± 0.12^{c}
TLT-2500	2.05 ± 0.03^{ab}	63.45 ± 0.03^{d}	336.14 ± 4.68^{c}	3.21 ± 0.26^{a}	91.29 ± 0.24^{b}	5.50 ± 0.02^{d}
TLT-3000	2.06 ± 0.04^{ab}	63.45 ± 0.02^{d}	460.66 ± 11.96^{ab}	3.19 ± 0.18^{a}	90.44 ± 0.20^{c}	6.36 ± 0.17^{c}

Different lowercase letters indicate significant differences ($P < 0.05$).

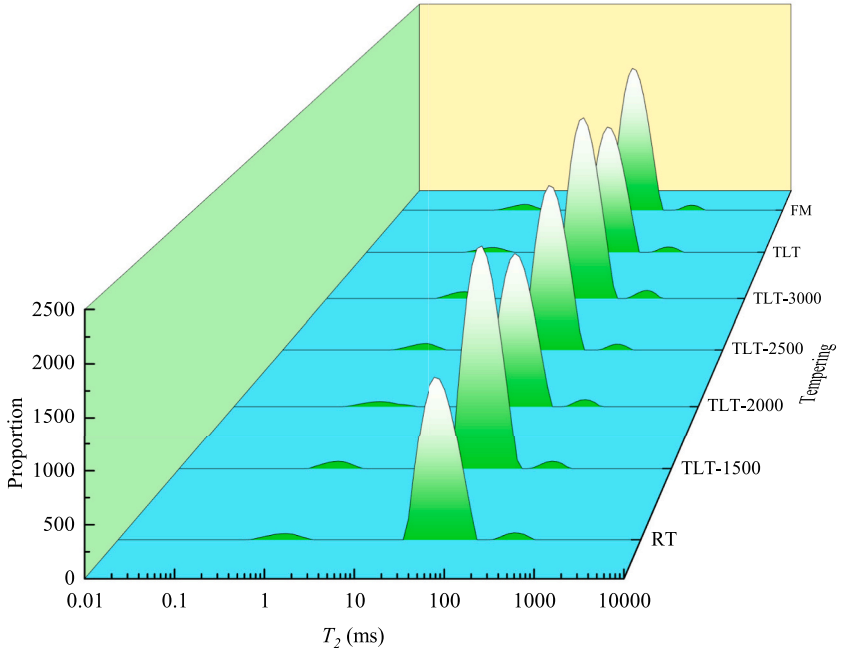

Fig. 5. Changes in moisture distribution and migration of tan mutton under different tempering strategies.

minimal free water content among all tempering groups. Conversely, the most notable decrease and increase ($P < 0.05$) in P_{22} and P_{23} occurred in RT relative to FM, indicating a greater conversion of immobile water to free water during RT. This finding is consistent with the water retention analysis of Tan mutton in Section 3.2. When combined with observations of muscle tissue in Section 3.4.1 and subsequent analysis of textural properties in Section 3.4.2, it suggests that the tempering process, particularly prolonged RT, led to muscle tissue degradation, weakened water retention ability, and diminished protein-water binding due to oxidative denaturation (Zhu et al., 2021). Consequently, immobile water in Tan mutton gradually transitioned to free water, resulting in juice loss.

3.7. Lipid oxidation

Tan mutton is rich in a diverse array of unsaturated fatty acids, susceptible to auto-oxidation or lipoxygenase activity, yielding primary oxidation products like conjugated dienes and hydroperoxides, subsequently leading to the formation of aldehydes and ketones, imbued with distinctive odors. Among these oxidation products, malondialdehyde (MDA) can react with TBA to yield a stable red compound, with the absorbance of this compound demonstrating a linear correlation with MDA concentration within a defined range (Mousakhani-Ganjeh et al., 2016b). Consequently, the absorbance value of the resultant compound serves as an indicator for assessing the extent of fat oxidation and rancidity in Tan mutton.

As depicted in Fig. 6, FM exhibited the lowest TBARS value at 0.15 nmol/mgProt, whereas TBARS values for RT, TLT, TLT-1500, TLT-2000, TLT-2500, and TLT-3000 were recorded at 0.45, 0.37, 0.23, 0.16, 0.20, and 0.22 nmol/mgProt, respectively. Tukey's multiple comparisons analysis revealed a significant elevation in TBARS values for all tempering groups compared to FM ($P < 0.05$), except for TLT-2000, which did not significantly differ from FM ($P > 0.05$). RT exhibited the highest TBARS values among the groups, possibly attributed to prolonged tempering at room temperature, resulting in increased oxygen exposure to Tan mutton, consequently promoting extensive fat oxidation (Zhou & Xie., 2021). Furthermore, protein and lipid oxidation typically coincide with reduced muscle protein functionality, manifested by diminished WRC and weakened gel strength. Partial loss of juice not only leads to water and soluble protein loss but also releases fat

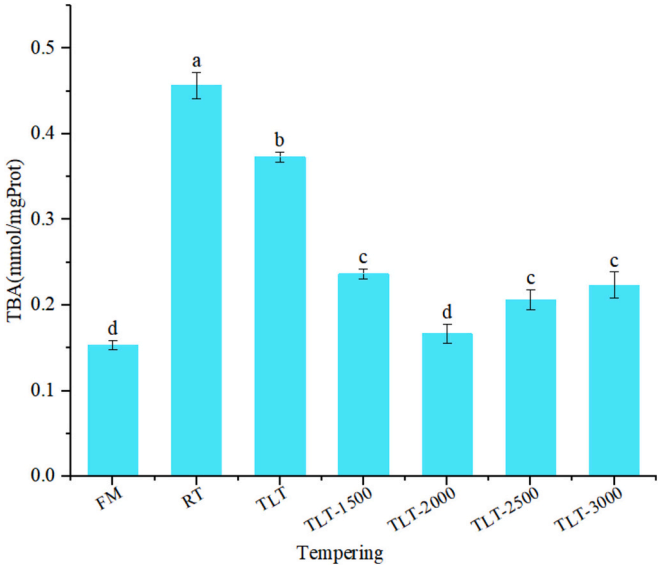

Fig. 6. Changes in lipid oxidation of tan mutton under different tempering strategies. Different lowercase letters indicate significant differences ($P < 0.05$), while error bars show standard deviation.

oxidation precursors, notably free iron ions, which facilitate electron transfer reactions with molecular oxygen, thereby promoting lipid oxidation (Du et al., 2022). Additionally, prolonged tempering-induced ice crystal activity disrupts muscle tissue cells, denaturing and deactivating crucial antioxidant enzymes, while also releasing fat oxidation promoters such as Fe^{2+}, further accelerating lipid oxidation. In addition, there is a certain dependency between protein oxidation and lipid oxidation, where protein oxidation proceeds while lipid oxidation is occurring, and the ensuing intermediates from lipid oxidation, such as peroxides, react with proteins to form complexes and further promote lipid oxidation (Cai et al., 2020).

In contrast to RT, TLT, and low-voltage electrostatic fields significantly ($P < 0.05$) reduced the lipid oxidation in Tan mutton, with lipid oxidation decreasing progressively as the electrostatic field intensity increased. Combining this with the analysis of the tempering-temperature curve in Section 3.1 and the TVB-N value in Section 3.3.3, it can be concluded that TLT and electrostatic fields expedite the tempering process and reduce the exposure time of mutton to oxygen. Additionally, the lower temperature inhibits the progression of lipid oxidation (Jia, Liu, et al., 2017). Furthermore, TLT and electrostatic field tempering reduced tempering loss, thereby minimizing the exposure of lipid pro-oxidants and lipid oxidation precursors to juice loss, subsequently slowing down lipid oxidation. However, a significant increase in TVB-N values of Tan mutton was observed when the electric field exceeded 2000 V. This may be attributed to the increased strength of electrostatic field that intensifies air ionization and elevates the concentration of ozone, which subsequently leads to enhanced lipid oxidation on the surface of the Tan mutton (Amiri et al., 2019).

3.8. Color and luster

The color and luster of meat products are critical factors influencing consumer purchase decisions, as these attributes serve as indicators of freshness and quality, directly affecting consumer desire. As shown in Table 2, the L^* and a^* values of Tan mutton experienced a significant decrease after tempering, while the b^* values increased significantly ($P < 0.05$). The L^* value reflects the degree of light reflection from the sample, which is primarily influenced by the moisture content (Zhu et al., 2019). A higher loss of moisture leads to an increased refractive index on the sample surface, resulting in a lower L^* value. RT, with the poorest water retention, had the lowest L^* value, whereas TLT-2000 and TLT-2500, which had water retention comparable to FM, showed no significant change in L^* values ($P > 0.05$). Furthermore, Sun et al. (2021) stated that protein denaturation, fat oxidation, and pigment degradation during frozen storage and thawing also contribute to the decrease in the L^* value of meat products. This aligns with the findings in Section 3.6 on lipid oxidation: RT, with higher lipid oxidation, had lower L^* values, whereas TLT and electrostatic field-treated Tan mutton, with lower lipid oxidation, had higher L^* values.

Similar to the trend in L^* values, a^* values of Tan mutton in all groups decreased significantly ($P < 0.05$) compared to FM after tempering. Cai et al. (2020) stated that the a^* value of meat products is related to the content of myoglobin and hemoglobin, and the color of meat products mainly depends on the ratio of reduced myoglobin, oxymyoglobin, and

Table 2
Changes in L^*, a^*, b^* of tan mutton under different tempering treatments.

Tempering	L*	a*	b*
FM	29.30 ± 0.59^{a}	31.71 ± 1.02^{a}	11.93 ± 0.16^{e}
RT	20.03 ± 1.72^{d}	19.54 ± 0.67^{d}	22.54 ± 0.28^{a}
TLT	22.81 ± 0.19^{cd}	23.55 ± 1.60^{c}	21.34 ± 0.26^{bc}
TLT-1500	24.71 ± 1.10^{bc}	25.79 ± 0.83^{bc}	20.91 ± 0.51^{c}
TLT-2000	28.74 ± 0.11^{a}	27.43 ± 0.52^{b}	17.11 ± 0.08^{d}
TLT-2500	26.59 ± 0.94^{ab}	31.28 ± 1.18^{a}	17.65 ± 0.37^{d}
TLT-3000	25.24 ± 1.27^{bc}	26.29 ± 0.13^{b}	21.88 ± 0.37^{ab}

Different lowercase letters indicate significant differences ($P < 0.05$).

metmyoglobin (Met-Mb). Typically, myoglobin in meat exists as a reduced form of ferrimyoglobin, which combines with oxygen to form oxymyoglobin, giving the meat a bright red color. However, oxymyoglobin can be oxidized to Met-Mb under various conditions (temperature, time, and oxygen levels), leading to the browning of the meat (Cai et al., 2020). FM shows a bright red color due to its high oxymyoglobin content, but as oxymyoglobin oxidizes to Met-Mb, Tan mutton acquires a dark red color. As illustrated in Table 2, the a^* value in RT decreased most significantly ($P < 0.05$) compared to FM, whereas the a^* value in TLT-2500 was not significantly different from FM. The decrease in a^* values in RT may be attributed to prolonged tempering time, which increases oxygen exposure and myoglobin oxidation. Additionally, the WRC of Tan mutton weakened during RT, and Met-Mb reductase might have been lost with the exudate. In fresh muscle, Met-Mb reductase is highly active, quickly reducing Met-Mb back to deoxymyoglobin and maintaining muscle color. However, during tempering, Met-Mb reductase may be lost from the sarcoplasmic environment in the form of exudates, resulting in Met-Mb accumulation on the muscle surface and a significant reduction in a^* values. Conversely, TLT and electrostatic fields accelerated the tempering process and effectively inhibited myoglobin oxidation in Tan mutton, resulting in significantly higher a^* values than RT ($P < 0.05$). With the application of TLT and electrostatic fields, the a^* values gradually increased, reaching the FM level at TLT-2500. However, the a^* values of TLT-3000 decreased significantly ($P < 0.05$) compared to TLT-2000 and TLT-2500. This decrease could be attributed to excessive myoglobin oxidation due to the higher electrostatic field intensity, leading to the accumulation of Met-Mb (brown color) on the meat surface and subsequent browning of the Tan mutton (Sun et al., 2021).

In contrast to the distinct changes in L^* and a^* values, the b^* values of Tan mutton increased significantly ($P < 0.05$) after tempering. Among the tempering groups, only the b^* values of TLT-2000 and TLT-2500 were closest to the level of FM, while the b^* values of RT and other groups were substantially higher than those of FM. Fat oxidation during freezing and thawing induced a non-enzymatic browning reaction and accelerated the formation of yellow pigments, leading to higher b^* values in meat products. Similarly, D. Li et al. (2020), in their study of ultrasound-assisted thawing, air thawing, and water thawing of bighead carp, found that changes in b^* values were primarily related to the oxidation of abundant polyunsaturated fatty acids.

3.9. Correlation analysis

The correlation analysis between the quality indicators such as tempering time, tempering loss and cooking loss of Tan mutton under different tempering methods are presented in Supplementary material 2. The results showed that the tempering time had a highly significant ($P < 0.01$) effect on WRC (tempering loss, cooking loss and centrifugation loss), pH and T_{22}, and was negatively correlated with L^* and a^*. When the integrity of the muscle tissue is compromised, its ability to retain tissue fluids physically is impaired, weakening the WRC of the muscle tissue. Furthermore, the loss of tissue fluid affects muscle EC and pH, which in turn has a significant effect on lipid oxidation in Tan mutton ($P < 0.01$). This could be attributed to the lower WRC of Tan mutton, leading to more severe tissue fluid loss and disruption of ionic balance in the muscle tissue, resulting in significant changes in pH. Additionally, some conductive ionic compounds (including Fe^{2+} and other possible ions) may be present in this tissue fluid. The loss of these ionic compounds could lead to changes in the EC values of Tan mutton and may promote lipid oxidation, thereby affecting the TBARS values. Moreover, changes in the WRC of Tan mutton are highly correlated with its color and luster (L^*, a^*, b^*). This suggests that changes in the existence state and content of water in Tan mutton significantly influence the surface luster (L^*) and the oxidation of myoglobin (a^*). Additionally, from the analysis of lipid oxidation in Section 3.6, the loss of tissue fluid in Tan mutton may release lipid oxidase and oxidation promoters, leading to more severe fat oxidation in Tan mutton, which may be indicated by an elevated b^* value due to the yellow coloration produced by lipid oxidation.

4. Conclusions

The effects of TLT, TLT-1500/2000/2500/3000, and RT on the quality of Tan mutton were investigated in this study. TLT and TLT-1500/2000/2500/3000 significantly ($P < 0.05$) enhanced the tempering rate relative to RT, with the rate increasing significantly with the strength of the electrostatic field ($P < 0.05$). The lowest tempering loss and no significant differ in centrifugal loss ($P > 0.05$) to FM, indicating that TLT-2500 provided the best WRC. Further the pH of TLT-2500-treated Tan mutton was similar to FM, while the EC and TVB-N levels were close to those of FM, indicating that TLT-2500 better maintained the freshness of Tan mutton. The SEM revealed that all tempering treatments significantly damaged the muscle fiber integrity of Tan mutton, leading to textural deterioration. However, the muscle fiber integrity of TLT-2500-treated Tan mutton was closest to that of FM. The LF-NMR showed that TLT-2500-treated Tan mutton contained the highest amount of immobile water and the least amount of free water, exhibiting the best WRC. Additionally, in terms of lipid oxidation and color change, TLT-2500-treated Tan mutton was closest to FM. In conclusion, TLT-2500 maintained the quality of Tan mutton, highlighting its potential as a processing method in the meat industry.

CRediT authorship contribution statement

Yuanlv Zhang: Writing – review & editing, Writing – original draft, Validation, Software, Methodology, Investigation, Formal analysis. **Guishan Liu:** Writing – review & editing, Supervision, Funding acquisition, Conceptualization.

Declaration of competing interest

The authors declare that they have no known competing financial interests or personal relationships that could have appeared to influence the work reported in this paper.

Acknowledgments

The study was supported by the Key Research and Development Program in Ningxia Hui Autonomous Region in 2023 (Grant No. 2023BCF01041), the Science and Technology Planning Project of Yinchuan, Ningxia Province in 2022 (Grant No. 2022ZDNY05), the leading Talent Project of Science and Technology Innovation in Ningxia Hui Autonomous Region in 2020 (Grant No. 2020GKLRLX05), and the Key R&D Program Projects in Yanchi, Ningxia (Grant No. 2023YCYDCT009).

Appendix A. Supplementary data

Supplementary data to this article can be found online at https://doi.org/10.1016/j.fochx.2024.101926.

Data availability

Data will be made available on request.

References

Amiri, A., Mousakhani-Ganjeh, A., Shafiekhani, S., Mandal, R., Singh, A. P., & Kenari, R. E. (2019). Effect of high voltage electrostatic field thawing on the functional and physicochemical properties of myofibrillar proteins. *Innovative Food Science & Emerging Technologies, 56*, Article 102191. https://doi.org/10.1016/j.ifset.2019.102191

Bekhit, A. E.-D. A., Holman, B. W. B., Giteru, S. G., & Hopkins, D. L. (2021). Total volatile basic nitrogen (TVB-N) and its role in meat spoilage: A review. *Trends in Food Science & Technology, 109*, 280–302. https://doi.org/10.1016/j.tifs.2021.01.006

Cai, L., Wan, J., Li, X., & Li, J. (2020). Effects of different thawing methods on conformation and oxidation of myofibrillar protein from largemouth bass (*Micropterus salmoides*). *Journal of Food Science, 85*(8), 2470–2480. https://doi.org/10.1111/1750-3841.15336

Cai, L., Zhang, W., Cao, A., Cao, M., & Li, J. (2019). Effects of ultrasonics combined with far infrared or microwave thawing on protein denaturation and moisture migration of Sciaenops ocellatus (red drum). *Ultrasonics Sonochemistry, 55*, 96–104. https://doi.org/10.1016/j.ultsonch.2019.03.017

Cao, M., Cao, A., Wang, J., Cai, L., Regenstein, J., Ruan, Y., & Li, X. (2018). Effect of magnetic nanoparticles plus microwave or far-infrared thawing on protein conformation changes and moisture migration of red seabream (*Pagrus Major*) fillets. *Food Chemistry, 266*, 498–507. https://doi.org/10.1016/j.foodchem.2018.06.057

Chen, S., Wu, W., Yang, Y., Wang, H., & Zhang, H. (2020). Experimental study of a novel vacuum sublimation–rehydration thawing for frozen pork. *International Journal of Refrigeration, 118*, 392–402. https://doi.org/10.1016/j.ijrefrig.2020.06.004

Cheng, H., Bian, C., Chu, Y., Mei, J., & Xie, J. (2022). Effects of dual-frequency ultrasound-assisted thawing technology on thawing rate, quality properties, and microstructure of large yellow croaker (*Pseudosciaena crocea*). *Foods, 11*(2), 16. Article 226 https://doi.org/10.3390/foods11020226.

Du, X., Wang, B., Li, H., Liu, H., Shi, S., Feng, J., et al. (2022). Research progress on quality deterioration mechanism and control technology of frozen muscle foods. *Comprehensive Reviews in Food Science and Food Safety, 21*(6), 4812–4846. https://doi.org/10.1111/1541-4337.13040

Hu, F., Qian, S., Huang, F., Han, D., Li, X., & Zhang, C. (2021). Combined impacts of low voltage electrostatic field and high humidity assisted-thawing on quality of pork steaks. *LWT, 150*, Article 111987. https://doi.org/10.1016/j.lwt.2021.111987

Jia, G., He, X., Nirasawa, S., Tatsumi, E., Liu, H., & Liu, H. (2017). Effects of high-voltage electrostatic field on the freezing behavior and quality of pork tenderloin. *Journal of Food Engineering, 204*, 18–26. https://doi.org/10.1016/j.jfoodeng.2017.01.020

Jia, G., Liu, H., Nirasawa, S., & Liu, H. (2017). Effects of high-voltage electrostatic field treatment on the thawing rate and post-thawing quality of frozen rabbit meat. *Innovative Food Science & Emerging Technologies, 41*, 348–356. https://doi.org/10.1016/j.ifset.2017.04.011

Jia, G., van den Berg, F., Hao, H., & Liu, H. (2020). Estimating the structure of sarcoplasmic proteins extracted from pork tenderloin thawed by a high-voltage electrostatic field. *Journal of Food Science and Technology, 57*(4), 1574–1578. https://doi.org/10.1007/s13197-020-04253-4

Lan, W., Zhao, Y., Gong, T., Mei, J., & Xie, J. (2021). Effects of different thawing methods on the physicochemical changes, water migration and protein characteristic of frozen pompano (*Trachinotus ovatus*). *Journal of Food Biochemistry, 45*(8), Article e13826. https://doi.org/10.1111/jfbc.13826

Lee, S., Kim, E. J., Park, D. H., & Choi, M.-J. (2021). Two-stage air thawing as an effective method for controlling thawing temperature and improving the freshness of frozen pork loin. *LWT, 140*, Article 110668. https://doi.org/10.1016/j.lwt.2020.110668

Li, D., Zhao, H., Muhammad, A. I., Song, L., Guo, M., & Liu, D. (2020). The comparison of ultrasound-assisted thawing, air thawing and water immersion thawing on the quality of slow/fast freezing bighead carp (*Aristichthys nobilis*) fillets. *Food Chemistry, 320*, Article 126614. https://doi.org/10.1016/j.foodchem.2020.126614

Li, F., Wang, B., Liu, Q., Chen, Q., Zhang, H., Xia, X., & Kong, B. (2019). Changes in myofibrillar protein gel quality of porcine longissimus muscle induced by its stuctural modification under different thawing methods. *Meat Science, 147*, 108–115. https://doi.org/10.1016/j.meatsci.2018.09.003

Li, F., Zhu, Y., Li, S., Wang, P., Zhang, R., Tang, J., et al. (2021). A strategy for improving the uniformity of radio frequency tempering for frozen beef with cuboid and step shapes. *Food Control, 123*, Article 107719. https://doi.org/10.1016/j.foodcont.2020.107719

Li, J., Shi, J., Huang, X., Zou, X., Li, Z., Zhang, D., et al. (2020). Effects of pulsed electric field on freeze-thaw quality of Atlantic salmon. *Innovative Food Science & Emerging Technologies, 65*, Article 102454. https://doi.org/10.1016/j.ifset.2020.102454

Li, Y., Jia, W., Zhang, C. H., Li, X., Wang, J. Z., Zhang, D. Q., & Mu, G. F. (2014). Fluctuated low temperature combined with high-humidity thawing to reduce physicochemical quality deterioration of beef. *Food and Bioprocess Technology, 7*(12), 3370–3380. https://doi.org/10.1007/s11947-014-1337-3

Llave, Y., & Erdogdu, F. (2022). Radio frequency processing and recent advances on thawing and tempering of frozen food products. *Critical Reviews in Food Science and Nutrition, 62*(3), 598–618. https://doi.org/10.1080/10408398.2020.1823815

Lv, Y., & Xie, J. (2022). Quality of cuttlefish as affected by different thawing methods. *International Journal of Food Properties, 25*(1), 33–52. https://doi.org/10.1080/10942912.2021.2019269

Mousakhani-Ganjeh, A., Hamdami, N., & Soltanizadeh, N. (2016a). Effect of high voltage electrostatic field thawing on the lipid oxidation of frozen tuna fish (*Thunnus albacares*). *Innovative Food Science & Emerging Technologies, 36*, 42–47. https://doi.org/10.1016/j.ifset.2016.05.017

Mousakhani-Ganjeh, A., Hamdami, N., & Soltanizadeh, N. (2016b). Thawing of frozen tuna fish (*Thunnus albacares*) using still air method combined with a high voltage electrostatic field. *Journal of Food Engineering, 169*, 149–154. https://doi.org/10.1016/j.jfoodeng.2015.08.036

Peng, Z., Zhu, M., Zhang, J., Zhao, S., He, H., Kang, Z., et al. (2021). Physicochemical and structural changes in myofibrillar proteins from porcine longissimus dorsi subjected to microwave combined with air convection thawing treatment. *Food Chemistry, 343*, Article 128412. https://doi.org/10.1016/j.foodchem.2020.128412

Qian, S., Li, X., Wang, H., Mehmood, W., Zhong, M., Zhang, C., & Blecker, C. (2019). Effects of low voltage electrostatic field thawing on the changes in physicochemical properties of myofibrillar proteins of bovine longissimus dorsi muscle. *Journal of Food Engineering, 261*, 140–149. https://doi.org/10.1016/j.jfoodeng.2019.06.013

Rahbari, M., Hamdami, N., Mirzaei, H., Jafari, S. M., Kashaninejad, M., & Khomeiri, M. (2018). Effects of high voltage electric field thawing on the characteristics of chicken breast protein. *Journal of Food Engineering, 216*, 98–106. https://doi.org/10.1016/j.jfoodeng.2017.08.006

Sun, Q., Kong, B., Liu, S., Zheng, O., & Zhang, C. (2021). Ultrasound-assisted thawing accelerates the thawing of common carp (*Cyprinus carpio*) and improves its muscle quality. *LWT, 141*, Article 111080. https://doi.org/10.1016/j.lwt.2021.111080

Wang, B., Bai, X., Du, X., Pan, N., Shi, S., & Xia, X. F. (2022). Comparison of effects from ultrasound thawing, vacuum thawing and microwave thawing on the quality properties and oxidation of porcine *longissimus Lumborum. Foods, 11*(9), 17. article 1368 https://doi.org/10.3390/foods11091368.

Wang, Z. T., Guan, X. Y., Mao, Y. X., Li, R., & Wang, S. J. (2023). Developing cold air assisted radio frequency tempering protocol based on heating rate, uniformity, and quality of frozen chicken breast. *Journal of Food Engineering, 340*, 9, 111302 https://doi.org/10.1016/j.jfoodeng.2022.111302.

Yao, H., Jin, Y., Zhang, X., Yang, N., & Xu, X. (2023). Influence of pulsed electric field on thawing of frozen pork: Physical properties, fat oxidation and protein structure. *Food Bioscience, 56*, Article 103175. https://doi.org/10.1016/j.fbio.2023.103175

Zhang, W., Cao, A., Shi, P., & Cai, L. (2021). Rapid evaluation of freshness of largemouth bass under different thawing methods using hyperspectral imaging. *Food Control, 125*, Article 108023. https://doi.org/10.1016/j.foodcont.2021.108023

Zhang, Y., Li, F., Yao, Y., He, J., Tang, J., & Jiao, Y. (2021). Effects of freeze-thaw cycles of Pacific white shrimp (*Litopenaeus vannamei*) subjected to radio frequency tempering on melanosis and quality. *Innovative Food Science & Emerging Technologies, 74*, Article 102860. https://doi.org/10.1016/j.ifset.2021.102860

Zhang, Y., Li, S., Jin, S., Li, F., Tang, J., & Jiao, Y. (2021). Radio frequency tempering multiple layers of frozen tilapia fillets: The temperature distribution, energy consumption, and quality. *Innovative Food Science & Emerging Technologies, 68*, Article 102603. https://doi.org/10.1016/j.ifset.2021.102603

Zhang, Y., Li, Y., Guo, J., Feng, Y., Xie, Q., Guo, M., et al. (2024). Effect of two-stage low-temperature tempering process assisted by electrostatic field application on physicochemical and structural properties of myofibrillar protein in frozen *longissimus dorsi* of tan mutton. *Food Chemistry, 456*, Article 140001. https://doi.org/10.1016/j.foodchem.2024.140001

Zhang, Y., Liu, G., Xie, Q., Wang, Y., Yu, J., & Ma, X. (2023a). A comprehensive review of the principles, key factors, application, and assessment of thawing technologies for muscle foods. *Comprehensive Reviews in Food Science and Food Safety, 22*(1), 107–134. https://doi.org/10.1111/1541-4337.13064

Zhang, Y., Liu, G., Xie, Q., Wang, Y., Yu, J., & Ma, X. (2023b). Physicochemical and structural changes of myofibrillar proteins in muscle foods during thawing: Occurrence, consequences, evidence, and implications. *Comprehensive Reviews in Food Science and Food Safety, 22*(4), 3444–3477. https://doi.org/10.1111/1541-4337.13194

Zhou, P., & Xie.. (2021). Effect of different thawing methods on the quality of mackerel (*Pneumatophorus japonicus*). *Food Science and Biotechnology, 30*(9), 1213–1223. https://doi.org/10.1007/s10068-021-00966-0

Zhu, M., Li, H., Xing, Y., Ma, C., Peng, Z., Jiao, L., et al. (2023). Understanding the influence of fluctuated low-temperature combined with high-humidity thawing on gelling properties of pork myofibrillar proteins. *Food Chemistry, 404*, Article 134238. https://doi.org/10.1016/j.foodchem.2022.134238

Zhu, M., Zhang, J., Peng, Z., Kang, Z., Ma, H., Zhao, S., et al. (2021). Fluctuated low temperature combined with high-humidity thawing to retain the physicochemical properties and structure of myofibrillar proteins from porcine *longissimus dorsi*. *LWT, 142*, Article 111001. https://doi.org/10.1016/j.lwt.2021.111001

Zhu, Y., Li, F., Tang, J., Wang, T., & Jiao, Y. (2019). Effects of radio frequency, air and water tempering, and different end-point tempering temperatures on pork quality. *Journal of Food Process Engineering, 42*(4), 8. e13026 https://doi.org/10.1111/jfpe.13026.